J|A|C|S ARTICLES

Published on Web 05/21/2010

The Membrane-Bound State of K_{2P} Potassium Channels

Werner Treptow*,† and Michael L. Klein*,‡

Laboratório de Biofísica, Departamento de Biologia Celular, Universidade de Brasília, Brasília, Brasil, and Institute for Computational Molecular Science, College of Science & Technology, Temple University, Philadelphia, Pennsylvania 19122

Received March 15, 2010; E-mail: treptow@unb.br; mlklein@temple.edu

Abstract: Potassium channel subunits composed of two-pore domains arranged in tandem (K_{2P}) are of paramount importance for neural function. A variety of stimuli, such as membrane depolarization and tension, acidification, and anesthetic action, activate K_{2P} channels. Most of the channel sensitivity is attributed to its intracellular C-terminal moiety, which works as a sensor domain required for proper integration of the electrical, chemical, and mechanical signals into channel activity. Herein, the structure of K_{2P} in a membrane environment has been studied using molecular dynamics (MD). Two distinct fully atomistic models for the most studied K_{2P} channel, namely, the TWIK-related (TREK)-1 channel have been built. These constructs were then inserted into a fully hydrated zwitterionic lipid bilayer, and each relaxed by means of MD simulations spanning $\sim$0.3 μs. Both simulated TREK-1 structures converged to a final conformation characterized by a closed pore and a C-terminal domain adsorbed onto the lipid bilayer surface. The C-terminus, which is physically linked to the pore and energetically coupled to the bilayer, is poised to gate the channel in response to membrane stimulation. The present study indicates the nature of the direct coupling between the C-terminal domain and the membrane, which is a key structural feature underlying K_{2P} channel function.

Introduction

Potassium channels are transmembrane (TM) proteins that aid the transport of K^+ ions across biological membranes. Members of the most recently identified class of K^+ channels, the two-pore domain (K_{2P}), are of paramount importance for neural function.[1] Setting the resting potential of the cell, K^+ homeostasis, mechanoreception, oxygen/pH sensing, anesthesia and neuroprotection against a range of neuronal diseases, including epilepsy, pain[2] and depression,[3] are some of the tasks attributed to K_{2P}.

The functional versatility of K_{2P} channels results from their exquisite sensitivity to a variety of stimuli. Membrane stretch[4] and depolarization,[5,6] warm temperature,[7] pH variations,[8,9] polyunsaturated fatty acids[4] and phospholipids[10] can activate (open) members of the K_{2P} family. The gating of K_{2P} channels can be further modulated by second messengers coupled to TM receptors via protein kinases,[4,11] by intracellular polylysines and polyamines,[10] and by pharmacological agents, such as, volatile and gaseous general anesthetics.[12]

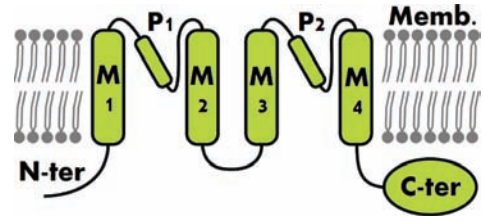

Figure 1. Topology of K_{2P} channels in the membrane. Within the TM region, the segments M1 through M2 and M3 through M4 form, respectively, the first and the second pore domain of TREK-1.

K_{2P} channels are complex quaternary structures with two-fold symmetry.[13] The main pore for ionic conduction results from the assembly of two TM domains, each expected to contain four helical segments, M1−M4, corresponding to an arrangement *in tandem* of two Pore domains (Figure 1). The protein N- and C-termini form intracellular domains, the latter being required for proper integration of the electrical,[5] chemical, and

† Universidade de Brasília.
‡ Temple University.

(1) Honoré, E. *Nat. Rev. Neurosci.* **2007**, *8*, 251–261.
(2) Alloui, A.; et al. *EMBO J.* **2006**, *25*, 2368–2376.
(3) Heurteaux, C.; Lucas, G.; Guy, N.; El Yacoubi, M.; Thümmler, S.; Peng, X. D.; Noble, F.; Blondeau, N.; Widmann, C.; Borsotto, M.; Gobbi, G.; Vaugeois, J. M.; Debonnel, G.; Lazdunski, M. *Nat. Neurosci.* **2006**, *9*, 1134–1141.
(4) Patel, A. J.; Honoré, E.; Maingret, F.; Lesage, F.; Fink, M.; Duprat, F.; Lazdunski, M. *EMBO J.* **1998**, *17*, 4283–4290.
(5) Maingret, F.; Honoré, E.; Lazdunski, M.; Patel, A. J. *Biochem. Biophys. Res. Commun.* **2002**, *292*, 339–346.
(6) Bockenhauer, D.; Zilberberg, N.; Goldstein, S. A. *Nat. Neurosci.* **2001**, *4*, 486–491.
(7) Maingret, F.; Lauritzen, I.; Patel, A. J.; Heurteaux, C.; Reyes, R.; Lesage, F.; Lazdunski, M.; Honoré, E. *EMBO J.* **2000**, *19*, 2483–2491.
(8) Maingret, F.; Patel, A. J.; Lesage, F.; Lazdunski, M.; Honoré, E. *J. Biol. Chem.* **1999**, *274*, 26691–26696.
(9) Honoré, E.; Maingret, F.; Lazdunski, M.; Patel, A. J. *EMBO J.* **2002**, *21*, 2968–2976.
(10) Chemin, J.; Patel, A. J.; Duprat, F.; Lauritzen, I.; Lazdunski, M.; Honoré, E. *EMBO J.* **2005**, *24*, 44–53.
(11) Murbartián, J.; Lei, Q.; Sando, J. J.; Bayliss, D. A. *J. Biol. Chem.* **2005**, *280*, 30175–30184.
(12) Patel, A. J.; Honoré, E.; Lesage, F.; Fink, M.; Romey, G.; Lazdunski, M. *Nat. Neurosci.* **1999**, *2*, 422–426.
(13) Lesage, F.; Guillemare, E.; Fink, M.; Duprat, F.; Lazdunski, M.; Romey, G.; Barhanin, J. *EMBO J.* **1996**, *15*, 6400–6407.

mechanical[4,8,14] signals into channel's activity. How do K_{2P} channels function? To begin to answer this question, one needs to know not only the atomic structure of the channel in the membrane-bound state, but also it is crucial to decipher the "sensing" conformational motions of the C-terminal domain, which ultimately lead to gating of the ion-conduction pathway.

Here, the structure of K_{2P} channels in a membrane environment has been investigated via molecular dynamics (MD). First, atomistic models have been built for the mechano- and arachidonic acid-activated TWIK related (TREK)-1 channel, the most studied member of the K_{2P} class.[1] The model constructs were embedded, and then relaxed, in a lipid bilayer using MD.

Methods

Primary Sequence Analysis of TREK-1. The primary sequence of the TREK-1 channel (gene name: ***KCNK2***) was taken from the Swiss-Prot server, entry number P97438. According to the HMMTOP algorithm,[15] the TM domain was predicted to include residues $N^{40}-S^{300}$. Helical segments within the TM domain and the secondary structure content within the N- and the C-terminal domains of TREK-1 were predicted using the JPRED server.[16]

Building the TREK-1 Homology Model. Piece-wise decomposition into domains is a typical approach to probe structure−function relationships in TM proteins.[17] The N-terminal domain of TREK-1 was shown to have no effects on any aspects of the protein function.[4,5,7,10,12,14] Thus, a truncated form of the channel was modeled, which comprised only the TM and the C-terminal domains. The strategy consisted of building separately a molecular model for each domain and subsequently merging them into a combined construct.

With the aid of comparative protein modeling,[18] homologous candidate structures (templates) for each of the domains were searched for in the Protein Data Bank (PDB) using the sequence-search module available on the data bank Web site. This module employs the FASTA algorithm[19] to align the primary sequence of unknown structure with the primary sequence of deposited structures in the bank, returning a list of templates classified according to the similarity with the query. Typically, homologous structures share a significant level of primary sequence similarity within regions of the tertiary structure primarily formed by α-helices and β-sheets compared to disordered extensions in coils. The output returned by the PDB search was then further refined manually in order to optimize the sequence alignment between TREK-1 and the templates inside the secondary structure segments of the channel.[18] From this procedure, the templates sharing the highest sequence similarity with TREK-1 were selected for use.

As in previous efforts,[20] the crystal structure of the *bacterial* KcsA channel from *Streptomyces lividans*[21] was the template for building the TM region of TREK-1 in the closed state. Among the K^+ channel structures available in the PDB, KcsA was found to share the highest sequence similarity (∼70.5%) within the helical segments of the TM domain of TREK-1 (Figure S1 and Table S1). According to the sequence alignment presented in Figure S1, the coordinates of two adjacent monomers in the KcsA crystal structure,[21] arranged in a clockwise orientation when viewed from the extracellular side, were then assigned to TREK-1. No accurate templates for modeling the external M1P1 loop of TREK-1 could be found in the PDB. The M1P1 loop is predicted to form a long coil of 60 amino acids comprising residues $E^{69}-L^{129}$. Given that this loop is not required for the structure stability and proper function of K_{2P} channels in the lipid-embedded state,[13] we mutated the M1P1 region in order to match the corresponding external loop in KcsA.

The C-terminal domain of TREK-1 seems to be very unique in the large family of K^+ channels. Members of the family possessing a C-terminal domain and for which crystal structures are available in the PDB (e.g., KcsA and KirBac) do not exhibit significant homology with the C-terminus of TREK-1. To build the C-terminal domain, the X-ray structure of the phosphate-acetyltransferase (ACTR) from *Bacillus subtilis*[22] was selected as a framework. In the PDB, this template shares the highest sequence similarity (∼54%) within the C-terminal segments of TREK-1 predicted to have secondary structure, and ∼66% within the coil extensions along the domain.

Although the TM domain of TREK-1 was experimentally predicted to dimerize when embedded in the membrane,[13] the oligomeric state of the C-terminal domain in the functional channel is still unknown. So, two distinct starting constructs, models 1 and 2, were built taking into consideration monomer and dimer configuration states of the C-terminus, respectively (Figure S2). The X-ray structure of the ACTR template was determined for the dimeric conformation of the protein, thus, also providing a structural framework to build the C-terminal as a dimer. Accordingly, in model 1, the C-terminal was merged with the TM domain by modeling the entire H1 segment as a helix-coil-helix structure. Differently, in model 2, the entire H1 segment was modeled in a α-helix, thereby placing further apart the C-terminal domains of the channel. We used the Modeler software (http://salilab.org/modeller/) for generating the TREK-1 starting models.

Building the Macromolecular System. After conformational energy minimization, each of the TREK-1 models was embedded in a fully hydrated lipid bilayer for subsequent refinement by means of MD simulation (Figure S3). The channel was inserted at the center of a 1-palmytoil-2-oleoyl-*sn*-glycero-3-phosphatidylcholine (POPC) patch, optimizing the distance between conserved aromatic residues, located at the extremities of segments M1−M4, and the membrane lipid head groups. The macromolecular systems contained individually a total of ∼162 000 atoms, including the TREK-1 channel, ∼425 lipid molecules, ∼40 000 water molecules, 2 K^+ ions located in the selectivity filter, and 14 chloride counterions in solution. In both systems, we considered all the protein-charged amino acids in their full-ionized state (pH = 7.0).

Molecular Dynamics Simulations. The MD simulations were carried out in the NPT ensemble using the program NAMD2.[23] Periodic-boundary conditions (PBC) were employed. The equations of motion were integrated using a multiple time-step algorithm.[24] Short- and long-range forces were calculated every 1 and 2 time-steps, respectively, with a time step of 2.0 fs. Langevin dynamics and Langevin piston methods were applied to keep the temperature (300 K) and the pressure (1 atm) of the system fixed. Chemical bonds between hydrogen and heavy atoms were constrained to their equilibrium values. Long-range electrostatic forces were taken into account using the particle mesh Ewald (PME) approach.[25] The

(14) Kim, Y.; Gnatenco, C.; Bang, H.; Kim, D. *Pfluegers Arch.* **2001**, *442*, 952–960.
(15) Tusnády, G. E.; Simon, I. *J. Mol. Biol.* **1998**, *283*, 489–506.
(16) Cole, C.; Barber, J. D.; Barton, G. J. *Nucleic Acids Res.* **2008**, *36*, 197–201.
(17) Kreusch, A.; Pfaffinger, P. J.; Stevens, C. F.; Choe, S. *Nature* **1998**, *392*, 945–948.
(18) Zhang, Y.; Skolnick, J. *Proc. Natl. Acad. Sci. U.S.A.* **2005**, *102*, 1029–1034.
(19) Lipman, D. J.; Pearson, W. R. *Science* **1985**, *227*, 1435–1441.
(20) Buckingham, S. D.; Kidd, J. F.; Law, R. J.; Franks, C. J.; Sattelle, D. B. *Trends Pharmacol. Sci.* **2005**, *26*, 361–367.
(21) Uysal, S.; Vásquez, V.; Tereshko, V.; Esaki, K.; Fellouse, F. A.; Sidhu, S. S.; Koide, S.; Perozo, E.; Kossiakoff, A. *Proc. Natl. Acad. Sci. U.S.A.* **2009**, *106*, 6644–6649.
(22) Xu, Q. S.; Jancarik, J.; Lou, Y.; Kuznetsova, K.; Yakunin, A. F.; Yokota, H.; Adams, P.; Kim, R.; Kim, S. H. *J. Struct. Funct. Genomics* **2005**, *6*, 269–279.
(23) Phillips, J. C.; Braun, R.; Wang, W.; Gumbart, J.; Tajkhorshid, E.; Villa, E.; Chipot, C.; Skeel, R. D.; Kale, L.; Schulten, K. *J. Comput. Chem.* **2005**, *26*, 1781–1802.
(24) Izaguirre, J. A.; Reich, S.; D., S. R. *J. Chem. Phys.* **1999**, *110*, 9853–9864.
(25) Darden, T.; York, D.; Pedersen, L. *J. Chem. Phys.* **1993**, *98*, 10089–10092.

water molecules were described using the TIP3P model.[26] The simulation used the CHARMM22-CMAP force field with torsional cross-terms for the protein[27,28] and CHARMM27 for the phospholipids.[29] A united-atom representation was adopted for the acyl chains of the POPC lipid molecules.[30] Execution of NAMD2 was performed on 128 INTEL 64 processors of a BLADES linux cluster at the University of Illinois' National Center for Supercomputing Applications (NCSA) and on 384 AMD-Opteron processors (2.6 GHz) of a CRAY-XT3 system at the Pittsburgh supercomputer center. Analyses of the MD trajectory were performed with VMD.[31]

The channel models 1 and 2 were relaxed embedded in the membrane by means of two independent MD runs (simulations MD1 and MD2). Each run followed three consecutive steps: (i) membrane equilibration for ~8.0 ns with the channel's coordinates constrained harmonically around the starting structure. Constraints were applied only to backbone atoms within the secondary structure elements. This procedure ensured a uniform and tight distribution of lipid molecules around the protein without disturbing the initial conformation; (ii) pre-equilibration of the initial model's conformation for ~4 ns by releasing slowly the harmonic constraints from the N- to the C-terminal of the protein, in order to avoid spurious nonequilibrium effects on the structure, especially in the C-terminal domain; (iii) multi nanosecond relaxation of the full channel system by means of unconstrained MD simulation.

Estimation of the Adsorption Free Energy. The free-energy variation ΔG involved on the C-terminal adsorption onto the membrane is given by:

$$\Delta G = G(\lambda_b) - G(\lambda_{ub}) \quad (1)$$

in which, λ_{ub} and λ_b denote the domain position along a reaction coordinate λ when it is, respectively, "unbound" from and adsorbed onto the membrane.

In the thermodynamic integration (TI) scheme, ΔG is obtained by integrating:

$$dG = \left\langle \frac{\partial V(X)}{\partial \lambda} \right\rangle_\lambda d\lambda = -\langle F_\lambda \rangle_\lambda \, d\lambda \quad (2)$$

where $V(X)$ is the potential energy of the domain for a given atomic configuration X, andF_λ is the derived force acting on the domain at a given position of the reaction coordinate. The brackets $\langle \, \rangle_\lambda$denote the mean value at the position λ.

The force F_λ can be decomposed in terms of the derived forces F_λ^i acting on the C-terminal amino acids i along the reaction coordinate, that is, $F_\lambda = \sum_i F_\lambda^i$. Accordingly, eq 2 can be rewritten as:

$$dG = -\langle \sum_i F_\lambda^i \rangle_\lambda \, d\lambda = -\sum_i \langle F_\lambda^i \rangle_\lambda \, d\lambda = \sum_i dG^i \quad (3)$$

or by integration,

$$\Delta G = \sum_i \Delta G^i \quad (4)$$

in which ΔG^i is the individual energy contribution of the C-terminal amino acid i to the adsorption free energy of the whole domain.

Here, we included in the estimation of ΔG only the *electrostatic* and *dispersion* nonbonded interactions between the domain and the headgroups of the internal surface of the lipid bilayer. One natural choice for λ was simply the distance Δz, along the TM direction, between the geometrical centers of the C-terminus and the lipid-head groups of the inner leaflet of the bilayer. From the MD trajectories 1 and 2, the force $F_{\lambda=\Delta z}$ was calculated using the *pair-interaction* module implemented in NAMD. The force $F_{\lambda=\Delta z}$ was then averaged over the reaction coordinate by considering bins of 0.1 Å, and subsequently integrated to provide the adsorption free-energy ΔG according to eq 2. The integration was taken over $\Delta z = -40$ and $\Delta z = -15$, corresponding, respectively, to the membrane unbound and bound states of the C-terminal (Figure 6). For estimation of the domain adsorption free-energy according to eq 4, $F^i_{\lambda=\Delta z}$ and ΔG^i for each of the C-terminal residues were computed using the same scheme above (Figure S5).

Results and Discussion

Each of the initial TREK-1 channel constructs (cf. Methods and Supporting Information), inserted in a fully hydrated and neutral (zwitterionic) phospholipid bilayer (Figure S3), was then relaxed by means of an independent MD trajectory spanning ~0.3 μs, at constant temperature (300 K) and pressure (1 atm), neutral pH, and with no applied TM electrostatic potential. For both of these simulations (MD1 and MD2), the membrane-bound channel stabilizes in a conformational state with a closed pore and each of the C-terminal subunits, denoted here as trk_1 and trk_2, adsorbed onto the lipid bilayer (Figure 2). Differences in the conformations obtained at the end of the MD simulations occur predominantly in the region of the C-terminal domain subunits (Table S2). Furthermore, since in the final structures the C-termini subunits (trk_1 and trk_2) are spatially decorrelated, the two MD runs can be viewed as generating four independent dynamical trajectories, which in turn yield four channel structures when symmetrized (Figure 3), namely, trk_1(MD1):trk_1(MD1); trk_2(MD1):trk_2(MD1); trk_1(MD2):trk_1(MD2); trk_2(MD2):trk_2(MD2). In the following, we consider each of the four structures to gain insights on the membrane-bound state of TREK-1.

The TM helical segments remained stable throughout the MD simulations (Figure S4). The root-mean-square deviation (rmsd) values for the whole TM domain as well as for the helical segments M1, P1, M2, M3, P2, and M4 range from 1.5 to 3.5 Å (Table S3), which agrees with the structural drift quantified in previous MD simulation studies of KcsA[32] and of other K^+ channels.[33,34] In contrast to the helical extensions within the TM region, the selectivity filter motif TTIGFG of TREK-1 diverged from its initial conformation. The relaxed structures exhibit a collapse at the location of the third K^+ site within the filter, resembling the structure of the selectivity filter of KcsA at low concentration of K^+.[35] Studies of the structure and conduction properties of the selectivity filter of TREK-1 are underway.

The structural stability of the TM segments was further reflected on the closed conformational state of the pore preserved during the simulations. In Figure 4, the leucine amino acids L_{174} (M2) and L_{289} (M4) close the channel pore, by delimiting the most constricted region of the ion permeation pathway, at the intracellular entrance of the protein. These residues in

(26) Jorgensen, W. L.; Chandrasekhar, J.; Madura, J. D.; Impey, R. W.; Klein, M. L. *J. Chem. Phys.* **1983**, *79*, 926–935.
(27) MacKerell Jr., A. D.; Feig, M.; Brooks III, C. L. *J. Am. Chem. Soc.* **2004**, *126*, 698–699.
(28) MacKerell, A. D., Jr.; et al. *J. Phys. Chem. B* **1998**, *102*, 3586–3616.
(29) Feller, S. E.; MacKerell, A. D., Jr. *J. Phys. Chem. B* **2000**, *104*, 7510–7515.
(30) Hénin, J.; Shinoda, W.; Klein, M. L. *J. Chem. Phys. B* **2008**, *112*, 7008–7015.
(31) Humphrey, W.; Dalke, A.; Schulten, K. *J. Mol. Graphics* **1996**, *14*, 33–38.
(32) Shrivastava, I. H.; Sansom, M. S. P. *Biophys. J.* **2000**, *78*, 557–570.
(33) Jogini, V.; Roux, B. *Biophys. J.* **2007**, *93*, 3070–3082.
(34) Treptow, W.; Tarek, M. *Biophys. J.* **2006**, *90*, L64–L66.
(35) Capener, C. E.; Proks, P.; Ashcroft, F. M.; Sansom, M. S. *Biophys. J.* **2003**, *84*, 2345–2356.

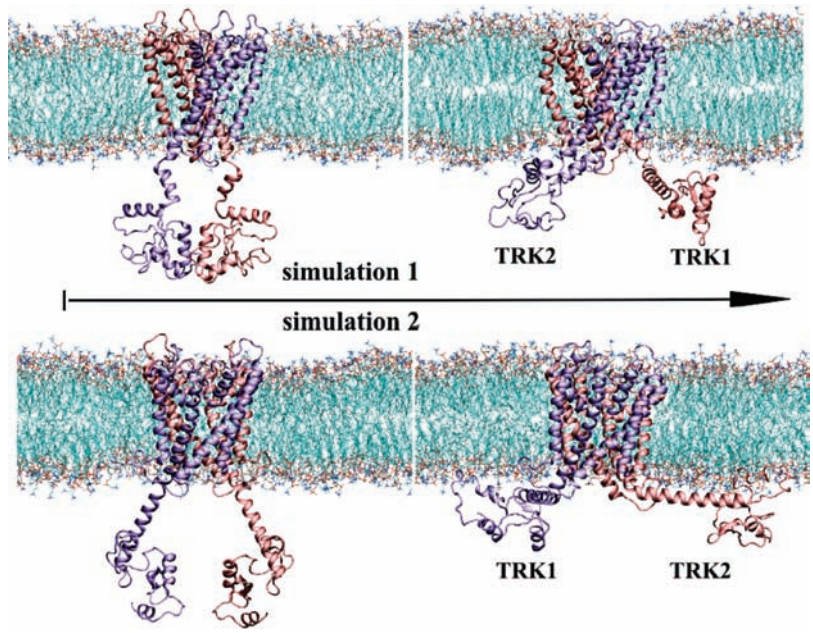

Figure 2. Initial (left) and final (right) conformational states of TREK-1 throughout simulations 1 and 2. Note the adsorption of the C-terminal domain onto the lipid bilayer for both of the channel subunits trk_1 and trk_2.

TREK-1 seem to form a hydrophobic gate that controls ion conduction, as previously reported for other K^+ channels.[36] The Leu gate likely forms one key constituent of the activation gate recently identified in K_{2P} channels.[37]

In contrast to the pore domain, the conformation of the C-terminal moiety diverged significantly from that of the initial constructs (Table S3). Each C-terminal subunit (trk_1 and trk_2) in both MD simulations relaxed to a final membrane-anchored state, persisting for the second half of the MD run (Figure 5A). The relaxed structures for the protein C-terminus present a good stereo chemical quality as confirmed by Procheck analyses.[38] A well-packed ensemble of secondary structures stabilizes their internal structure (Figure S4). Indeed, when bound to the bilayer, the rmsd profile for the C-terminal converges to a plateau value of less than 3.5 Å, indicative of structural stability of the domain (Figure 5B). In particular, for simulation MD1, the C-terminal subunits trk_1 and trk_2 dissociated from each other before membrane binding. Given the stochastic nature of this relaxation process, the C-terminus in trk_2 lost part of its secondary structure content in the final state.

The C-terminus interacts closely with the membrane by means of nonbonded electrostatic contacts between specific protein residues and the lipid bilayer head groups (Figure 5C,D). In Figure 6, we have estimated the adsorption free energy (ΔG) of the C-terminus onto the membrane due to the protein−lipid interactions (cf. Methods). In agreement with the dynamical process taking place in both simulations, these interactions favor significantly the domain adsorption as indicated by a $\Delta G = -654.3$ kcal·mol^{-1}. For all of the sampled conformations, the C-terminus proximal segment H1, comprising residues K_{301}−R_{330}, forms one major contact zone between the domain and the bilayer. Decomposition of ΔG in terms of the individual energy contributions arising from each of the C-terminal amino acids (ΔG^i) indicates that, for this segment, the energy accumulated over the constituent residues is $\sim$−385 kcal mol^{-1} (Figure 6D). This corresponds to $\sim$60% of the adsorption energy of the whole domain, indicating that the energetic coupling between the proximal region and the membrane is substantial. In Figure 3, the H1 segment, together with M4, forms an L-shaped helix-coil-helix structure at the main entrance of the pore. As a rigid helical structure physically linked to M4 and energetically coupled to the bilayer, the proximal region appears to form, therefore, a robust device able to gate the pore in response to membrane stretching. This is highly consistent with deletional and chimera analyses, showing the crucial role of the proximal region on the activation of TREK-1 by mechanical stimuli.[4,14]

The proximal region of the C-terminus is well-known to have a critical role on channel's activation induced by negatively charged phospholipids,[10,14] for example, the phosphatidylinositol-4,5-biphosphate, and by intracellular acidosis.[8,9] Clusters of basic (K_{301}, K_{302}, K_{304}, and R_{311}) and acidic (E_{305}, E_{306}, and E_{309}) amino acids located within the proximal region have been identified so far as the key molecular components attributing, respectively, lipid- and pH-sensitivity to TREK-1.[9] Here, by considering a neutrally charged zwitterionic lipid bilayer at neutral pH, we found these charged clusters in close proximity with lipids. As such, they contribute significantly to the adsorption energy of the C-terminal domain. Although having similar magnitude, their contribution is antagonistic, with the basic amino acids stabilizing the domain adsorption ($\Delta G^i < 0$).

These findings provide us with further insights on the state dependence of the channel with pH effects and lipids. Using the PROPKA empirical method for predicting protein pK_a,[39] we estimated the pK_a for the acidic residues E_{305}, E_{306}, and E_{309}. Their pK_a values, computed as averages over the ensemble of equilibrated channel conformations corresponding to the stable part of the trajectories, are 4.1 ± 4.0, 4.5 ± 4.7, and 5.7 ± 6.0,

(36) Treptow, W.; Tarek, M. *Biophys. J.* **2006**, *91*, L26–L28.
(37) Ben-Abu, Y.; Zhou, Y. F.; Zilberberg, N.; Yifrach, O. *Nat. Struct. Mol. Biol.* **2009**, *16*, 71–79.
(38) Laskowski, R. A.; MacArthur, M. W.; Moss, D. S.; Thornton, J. M. *J. Appl. Crystallogr.* **1993**, *26*, 283–291.
(39) Bas, D. C.; Rogers, D. M.; Jensen, J. H. *Proteins: Struct., Funct., Bioinf.* **2008**, *73*, 765–783.

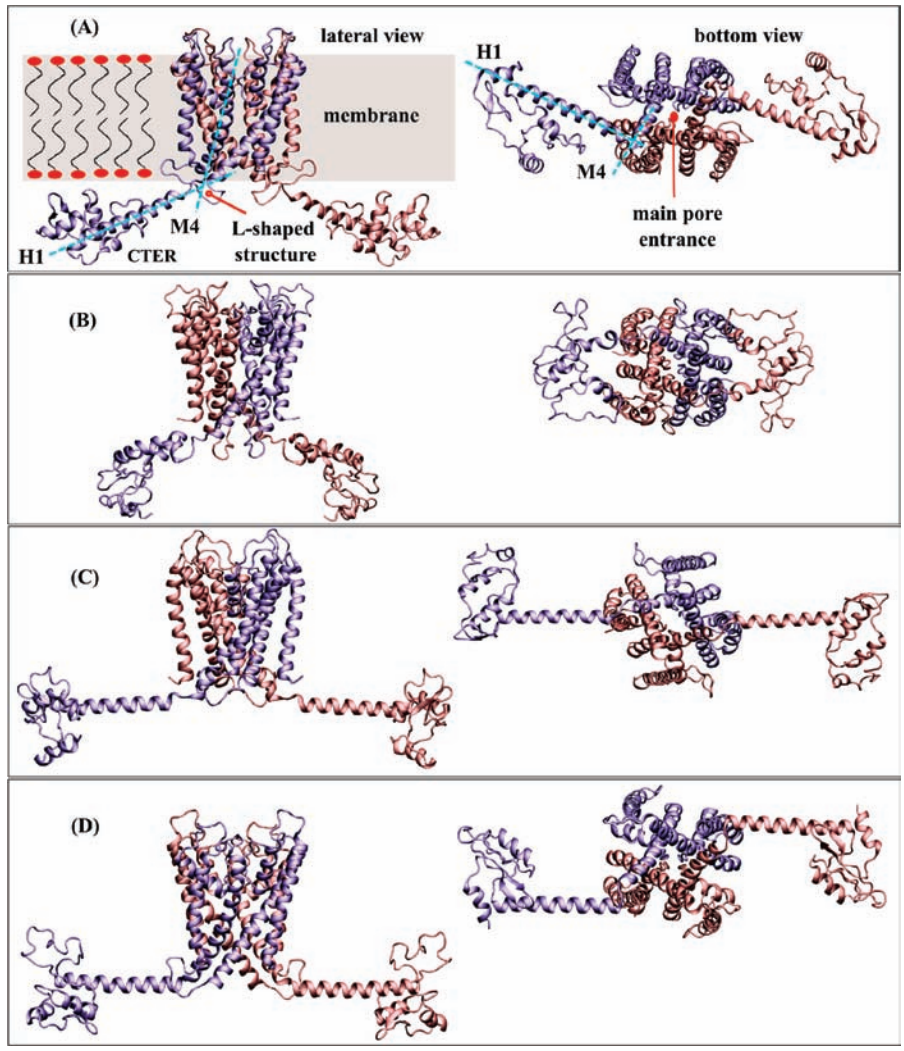

Figure 3. The membrane bound state of TREK-1. (A and B) Channel structures reconstructed, respectively, from the trk1 and trk2 conformations of simulation MD1. (C and D) Idem for simulation MD2. Note the L-shaped helix-coil-helix structure formed by M4 and the C-terminus proximal helix H1 at the internal pore entrance of the channel.

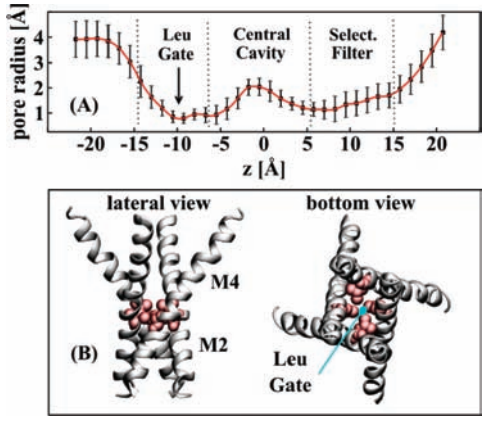

Figure 4. (A) Pore radius profile along the main pore of the channel. The profile is presented as a time average over the MD trajectories. Note that, in the Leu gate region, the pore radius is less than 1 Å, indicating the closure of the conduction pathway. The pore radius was calculated with HOLE.[19] (B) Structure of the main pore highlighting the Leu gate (red). For clarity, only segments M2 and M4 are shown.

respectively. These values are close to the reference pK_a for the glutamic amino acid free in solution (i.e., ~4.5), suggesting that protonation of E_{305}, E_{306}, and E_{309} would take place under acidification of the internal milieu. From the present analyses, one expects acidification (i.e., protonation of E_{305}, E_{306}, and E_{309}) to increase the coupling strength of H1 mediated by the basic amino acids K_{301}, K_{302}, K_{304}, and R_{311}. The structural modifications deriving from this modulation of the channel−membrane interactions could ultimately alter the conducting state of the pore. Indeed, the point mutation of E_{306} to alanine mimics the activation of the channel induced by acidification.[9]

Note that negatively charged lipids would likely also induce a similar structural effect on the channel, by increasing the coupling strength of H1 mediated by the basic amino acids K_{301}, K_{302}, K_{304}, and R_{311}. In the nicotinic acetylcholine receptor and voltage-sensor containing K^+ channels,[40,41] the interaction with specific lipid types, for example, cholesterol and phospholipids, is required for protein function. In these receptors, membrane-embedded regions of the protein form molecular cavities, with specific steric and electrostatic properties for lipid binding, a molecular feature that is absent in the C-terminal domain of TREK-1. As distinct from these receptors, the TREK-1 state

(40) Brannigan, G.; Hénin, J.; Law, R.; Eckenhoff, R.; Klein, M. L. *Proc. Natl. Acad. Sci. U.S.A.* **2008**, *105*, 14418–1423.
(41) Schmidt, D.; Jiang, Q. X.; MacKinnon, R. *Nature* **2006**, *444*, 775–779.

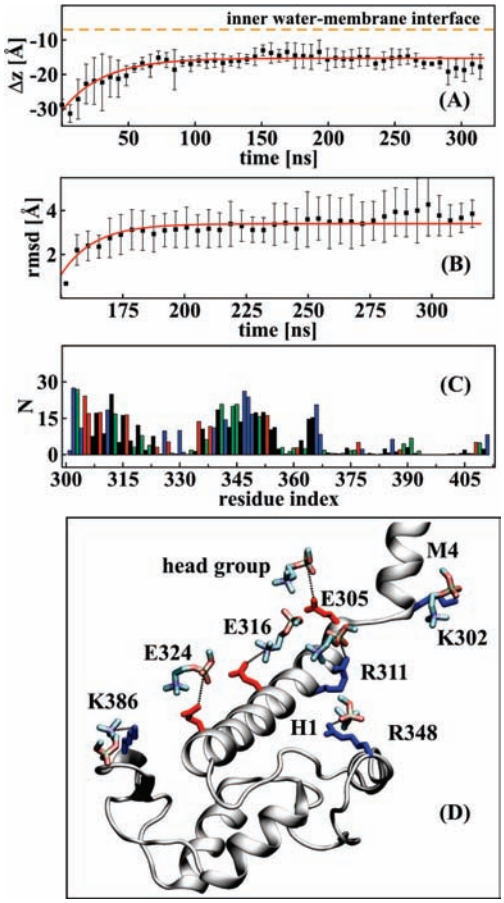

Figure 5. (A) Distance (Δz) between the geometrical centers of the C-terminal domain and of the lipid head groups of the inner leaflet of the bilayer. Δz is along the TM direction. The distance between both groups stabilizes around −15 Å within ∼100 ns, corresponding to the anchoring of the C-terminus to the membrane surface. (B) Root mean square deviation (rmsd) profile for the conformation of the C-terminal domain in the membrane-anchored state. Heavy atoms were included in the calculation, with the reference structure taken as the channel conformation at simulation time $t = 150$ ns. For (A) and (B), the data set is shown as an average over the simulations (black) and adjusted to one single exponential fit (red). (C) Radial distribution analysis showing the number (N) of lipid-headgroup atoms interacting with the C-terminus within a cutoff distance of 9 Å. Residues are colored according to their properties: basic (blue), acidic (red), polar (green), and nonpolar (black). (D) Close view of the C-terminus interacting with lipid head groups.

dependence on the nature of the membrane constituents seems therefore to be primarily related with a nonspecific electrostatic effect, which regulates the coupling between the C-terminal and the membrane. Further simulation studies by considering different lipid types will be required for a conclusive answer to this topic.

Bound to the membrane, the channel structure presents a network of intra- and intersubunit electrostatic interactions at the activation gate region, located at the intracellular entrance of the main conduction pore (Table 1). In this region, D_{179} belonging to segment M2 forms an intrasubunit salt bridge with K_{43} of segment M1. D_{179} also forms intersubunit salt bridges with R_{297} and K_{301} of segment M4. Beneath the activation gate region, E_{305}, E_{306}, and E_{309}, situated within the C-terminus proximal region, interacts with K_{45} belonging to segment M1. Similarly to other K^+ channels,[42] this salt-bridge network falling apart may also participate in the gating mechanism of TREK-1.

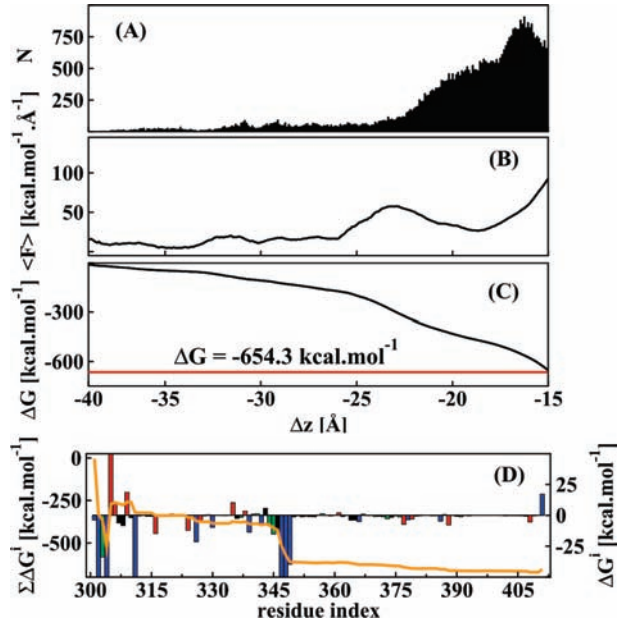

Figure 6. (A and B) Number of samples N and average force $\langle F \rangle$ along the reaction coordinate Δz. (C) Adsorption free energy (ΔG) of the C-terminus onto the membrane. The domain adsorption energy ($\Delta G = -654.3$ kcal·mol^{-1}) was computed by integrating $\langle F \rangle$ between the Δz positions −40 and −15 Å, which correspond, respectively, to the membrane unbound and bound states of the domain (cf. eqs 1 and 2). (D) Per residue energy variations ΔG^i contributing to ΔG (cf. eqs 3 and 4). Note that the cumulative energy variation $\sum \Delta G^i = -654.3$ kcal·mol^{-1} (orange line) is equal to the domain adsorption free-energy computed in panel C. Residues are colored according to their properties: basic (blue), acidic (red), polar (green), and nonpolar (black).

Table 1. Electrostatic Interactions at the Activation Gate Region of TREK-1

salt bridge pairs[a]	distance (Å)	salt bridge pairs	distance (Å)
D_{179}−K_{43} (IA)	3.3 ± 0.4	E_{305}−K_{45} (IR)	3.8 ± 1.5
D_{179}−K_{301} (IR)	10.1 ± 2.8	E_{306}−K_{45} (IR)	3.6 ± 1.2
D_{179}−R_{297} (IR)	9.4 ± 2.0	E_{309}−K_{45} (IR)	6.9 ± 1.8

[a] Determined for a cutoff distance of 3.2 Å between the oxygen atoms of acidic residues and the nitrogen atoms of basic residues. The distance values are presented as time averages over the simulations. IA and IR mean intra- and intersubunit, respectively.

Importantly, Figure 5C indicates that residues E_{335}−S_{370}, within the distal region of the C-terminus, form another major protein−lipid contact zone, which is contributing significantly to the adsorption of the domain (Figure 6D). This region superposes with the C-terminal segment (i.e., residues T_{363}−K_{411}) experimentally identified as playing an important role for channel gating induced by general anesthetics, such as chloroform and halothane.[12] Given that general anesthetics partition into the membrane and interact with channels in a protein-state dependent manner,[43,44] the present findings suggest an action mechanism in which the agonist affects channel pore gating via modulation of the C-terminal membrane coupling.

Conclusion

An atomistic structural description for the closed state of TREK-1 in a membrane environment is provided, which rationalizes the plethora of experimental findings on this and related channels.[4,5,7,8,10,14] As such, the MD study provides new directions for further experimental investigations. The crucial role of the leucine gate (L_{174} and L_{289}) on the gating machinery of TREK-1, as we propose, can be probed by testing experi-

(42) Craven, K. B.; Zagotta, W. N. *J. Gen. Physiol.* **2004**, *124*, 663–677.

mentally the channel ionic conductivity under site directed mutagenesis, similarly to previous assays performed on other potassium channels.[45] Double mutation experiments combined with electrophysiology measurements can be further employed to investigate the participation of the specific salt bridge pairs, herein identified, on the protein machinery.[42] One key result obtained from the present simulations relies on the critical role of the C-terminal domain on the channel activity, especially the fact that the domain involves a direct coupling with the membrane surface, especially the proximal region. This supports a mechanism in which chemical reagents, for example, lipids and anesthetics, alter the channel responsivity by modulating specifically the binding affinity of the C-terminus onto the membrane. If so, by attaching molecular probes located within the protein−lipid contact zones herein identified (Figure 5C), spectroscopy experiments should be highly sensitive to modifications of the protein membrane interactions under channel stimulation.

Given this, further structural and experimental studies aimed at the investigation of the dynamical processes underlying the membrane-stretch, pH, lipid, and anesthetic induced protein activation are within reach and should contribute to the deciphering of the key molecular mechanisms underlying the function of K_{2P} channels.

Acknowledgment. We thank Rob Eckenhoff, Grace Brannigan and Jérôme Hènin for useful discussions. Our research support came in part from the National Institutes of Health GM55876 and the National Science Foundation through TeraGrid resources.

Supporting Information Available: Molecular modeling, supplementary analyses, initial and final system configurations for simulations MD1 and MD2 (pdb.zip files). This material is available free of charge via the Internet at http://pubs.acs.org.

JA102191S

(43) Koubi, L.; Saiz, L.; Tarek, M.; Scharf, D.; Klein, M. L. *J. Phys. Chem. B* **2003**, *107*, 14500–14508.
(44) Vemparala, S.; Domene, C.; Klein, M. L. *Acc. Chem. Res.* **2010**, *43*, 103–110.
(45) Kitaguchi, T.; Sukhareva, M.; Swartz, K. J. *J. Gen. Physiol.* **2004**, *124*, 319–332.